16th World Conference on Earthquake, 16WCEE 2017
Santiago Chile, January 9th to 13th 2017
Paper N° 2126
Registration Code: S-G1464697230

3D DYNAMIC IMPEDANCES OF SURFACE FOOTINGS ON LIQUEFIABLE SOIL: EQUIVALENT LINEAR APPROACH

X. Karatzia[(1)], G. Mylonakis[(2)], G. Bouckovalas[(3)]

[(1)] Ph.D Candidate, Department of Civil Engineering, Univ. of Patras, Rio 26500, Greece, xkar@upatras.gr
[(2)] Professor, Dept. of Civil Engineering, Univ. of Bristol, Queens Building, Bristol BS8 1TR, U.K.; Professor, Dept. of Civil Engineering, Univ. of Patras, Rio 26500, Greece; Adjunct Professor, Univ. of California at Los Angeles, CA 90095, g.mylonakis@bristol.ac.uk
[(3)] Professor, School of Civil Engineering, NTUA, Greece, gbouck@central.ntua.gr

Abstract

Recent experimental and theoretical studies suggest that deep foundations may be avoided in a liquefaction regime, in the presence of a non-liquefiable layer on top of the liquefiable of adequate thickness and shear strength, which can restrain the accumulation of excessive seismic settlements and prevent post-shaking bearing capacity failure. This evidence has given rise to attempts for a complete design approach for the performance-based design of shallow foundations on liquefiable soils [1 – 3]. The design is based on the idea of a permeable crust (natural or artificial) which needs not extend over the whole depth of the liquefiable sand in order to take advantage of the observed benefits of settlement reduction [4, 5] at a reduced thickness and width. Within the above context the need arises to investigate the dynamic response of shallow foundations on liquefiable soils. The focus of the present study is upon the influence of liquefaction on the dynamic stiffness and damping ("impedance" functions) of rigid square footings resting on a multilayer soil profile involving a liquefiable layer, under external harmonic loading. To this end, a three-layer soil profile consisting of a surface clayey crust over a loose liquefiable sandy layer followed by a stiff impervious base stratum, are considered. The dynamic impedance of a rigid square footing is investigated parametrically using computer software CONAN [6], which is based on wave propagation in cones. A limited number of rigorous 3D numerical analyses with boundary elements [7] was also performed to check the accuracy of the cone models. Vertical, horizontal and rocking oscillations are considered. The results show that for common soil, foundation and seismic excitation conditions, liquefaction in the foundation soil leads to significant degradation of the dynamic spring coefficients and increase of the associated damping coefficients.

Keywords: dynamic impedance; surface footing; liquefiable soil; 3-layer soil profile

1. Introduction

In non-liquefiable soil profiles, soil-structure interaction in practical applications is traditionally considered by means of lumped springs and dashpots attached to the foundation. Contrary to approximate Winkler models employed for the analysis of piles and retaining walls, these formulations are usually rigorous, as the stiffness and damping coefficients are obtained from exact numerical solutions of the corresponding boundary value problems. Considering the importance of dynamic soil-structure interaction in earthquake and machine foundation problems, a vast set of analytical and numerical solutions for determining foundation impedances for footings of different shapes and soil stratification have been developed [8 – 13]. Published results refer to the common cases of a footing resting on a halfspace, on a soft or stiff layer overlying a halfspace [14], and a soil layer over rigid bedrock. Cases involving a smooth variation of soil properties with depth have also been considered [12, 13].

Clearly, such solutions are not applicable to liquefiable soils for two main reasons: a) the existence of a multi-layer soil profile (e.g. a non liquefiable surface crust – liquefiable soil layer – non liquefiable base stratum) with sharp impedance contrast between the layers, leading to the entrapment of seismic waves within the liquefied soil layer, and b) the mostly unknown mechanisms of seismic wave propagation within liquefied soil layers,

where shear-induced dilation under extremely low effective stresses leads to significant variation of excess pore pressure and seismic wave propagation velocity even within the same loading cycle.

The aim of this study is to investigate the dynamic impedance of a rigid surface square footing resting on a liquefiable sandy soil layer sandwiched between two stiff cohesive layers, under external harmonic loading. Results are obtained by means of elastodynamic analyses using pertinent values for the material constants. Key to analyzing a strongly non-linear phenomenon such as liquefaction using elastodynamic tools lies in the proper selection of shear wave propagation velocity during the course of liquefaction. There is ample experimental and analytical evidence that shear wave propagation velocity can be reduced to 10 – 30% of its initial value [15, 16] while at the same time the soil material damping ratio may increase to over 20%, in agreement with a substantial increase in imposed shear strains due to liquefaction. Based on the above observations, one may assess the effects of liquefaction through an equivalent linear elastic analysis using a low value of shear wave propagation velocity and a corresponding high value of hysteretic damping ratio for the liquefied soil stratum. Note that in the absence of sufficient soil permeability above and below the liquefied layer, this change in soil stiffness and damping may be considered to be "permanent" for the purposes of an earthquake dynamic analysis.

As a starting point, it is briefly recalled that the static stiffness of a rigid foundation in two dimensions may be expressed by means of appropriate stiffness coefficients, K^0_{ij}, corresponding to the foundation resistance to mode i for unit movement along the degree of freedom j (i.e., along the vertical, K^0_{vv}, horizontal, K^0_{hh}, rocking K^0_{rr}, and torsional, K^0_{tt}, degree of freedom). In the common case of combined action of a horizontal force and an overturning ("rocking") moment, the coupling term between horizontal and rocking mode K_{hr} is also present. Nevertheless, this coupling term is mainly significant for embedded foundations and, hence, it is omitted here. Furthermore, in the case of rigid foundations and linear or equivalent linear soil, static coefficients are functions of the soil shear modulus G, foundation width B, and soil Poisson's ratio v. For static conditions, the stiffness terms are written in the following dimensionally consistent form

$$K^0_{ij} = G\, B^m\, f_{ij}(v) \tag{1}$$

where K^0_{ij} stands for the force or moment along the degree of freedom i for a unit displacement or rotation along the degree of freedom j, while $m = 1$ for the translational degrees of freedom and $m = 3$ for the rotational. f_{ij} (v) is a dimensionless factor dependent solely on Poisson's ratio. In evaluating Eq. (1) in practical applications, the degradation of shear modulus due to increasing shear strain amplitude should be taken into account [17 – 19]. For small strains, the shear modulus, G_0, can be computed as

$$G_0 = V_s^{\,2}\, \rho \tag{2}$$

where V_s is the shear wave propagation velocity obtained by geophysical measurements and ρ is the soil mass density. For non-homogeneous soil, the usual practice is to compute an average effective value of V_s up to a certain depth, z_p, and then to correct this value according to the amplitude of deformation, as described in [19].

When the foundation is subjected to an external harmonic load with circular excitation frequency ω, for each oscillation mode (degree of freedom) the interacting soil-foundation system is represented by frequency-dependent springs and dashpots, as depicted in Fig. 1a. The frequency-dependence of the spring and dashpot coefficients stems from the elimination (condensation) of the infinite dynamic degrees of freedom in the soil. The dynamic impedance of foundation for each oscillation mode can thus be written in the generic form

$$S_{ij}\,(\omega) = K_{ij}\,(\omega) + i\omega C_{ij}\,(\omega) \tag{3}$$

where K_{ij} και C_{ij} are the dynamic stiffness and damping, respectively, and i is the imaginary unit ($\sqrt{-1}$), which indicates a phase lag of 90^o between the maximum spring force and the corresponding dashpot force.

It is common to describe frequency by means of the dimensionless coefficient $a_0 = \omega B/V_s$, where B refers to a foundation size parameter (typically full or half-width). This coefficient is interpreted as the ratio of B to 1/6 of wavelength λ for excitation frequency ω. Parameter a_0 is essentially unique for halfspace conditions (where B is the only parameter carrying units of length), but may not be ideal in the presence of bedrock at shallow depth

[20], or in the presence of a significantly stiffer surface soil crust as will be discussed in later sections. Alternatively, the dynamic impedance can be decomposed as

$$S_{ij}(a_0) = K^0_{ij}\,[\,k_{ij}(a_0) + i\,a_0\,c_{ij}(a_0)] \tag{4}$$

where K^0_{ij} is the static stiffness and k_{ij}, c_{ij} are dimensionless stiffness and damping coefficients, respectively, as a function of the dimensionless frequency a_0. The dimensionless stiffness and damping coefficients are real-valued. It is noted that, whereas the k_{ij} coefficient may also become negative at times (e.g. in case of phase lag between excitation and response greater than 90^o under dynamic conditions), c_{ij} is always a positive number so as to comply with thermodynamic constraints. It is mentioned that for a given foundation shape, the above dynamic impedance coefficients are functions of the Poisson's ratio v of the soil, the dimensionless frequency a_0, and the material damping ratio β.

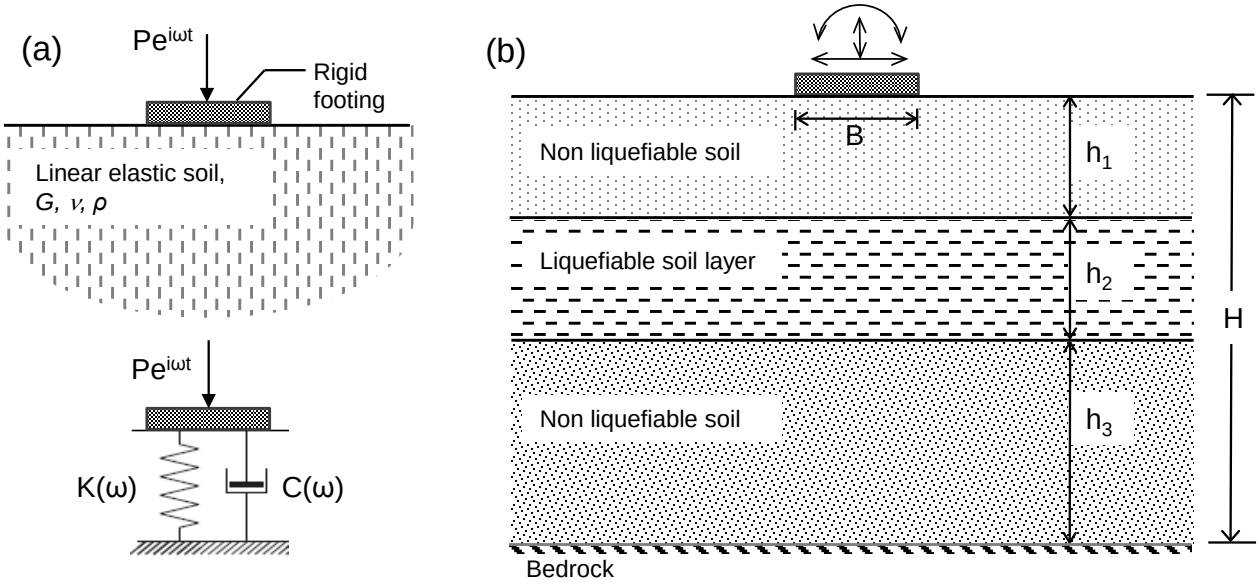

Fig. 1 – a) Physical interpretation of dynamic stiffness, b) Problem definition

2. Problem definition

The problem considered is depicted in Fig. 1b: a rigid surface footing on liquefiable soil subjected to harmonic loading. A three-layer soil profile consisting of a surface clayey crust overlying a liquefiable sandy layer followed by a stiff base stratum is considered. Owing to the sharp impedance contrast between these layers, which results in strong wave reflections, kinetic and potential energy is trapped within the profile in the form of stress waves. A numerical study for determining the dynamic impedance of the footing is conducted for three oscillation modes (vertical, horizontal and rocking). Numerical analyses refer to square footings of various sizes used for the foundation of both ordinary structures and bridge piers. Excitation frequencies cover the frequency range of importance in earthquake engineering.

To gain insight and provide comparisons, the elastodynamic analysis is performed in two stages: dynamic analysis without liquefaction and dynamic analysis with liquefaction, where the properties of the liquefiable soil stratum have been properly adjusted over those prior to liquefaction. As already mentioned, the principal parameter which needs to be degraded due to the occurrence of liquefaction and also dictates to a large extent the dynamic response of the footing, is the shear wave propagation velocity of the liquefiable sandy layer V_{sliq}. In the current analyses and except specifically otherwise indicated, it is assumed that V_{sliq} = 25m/s.

With reference to material damping of the liquefied soil, it has been observed that the energy loss due to material damping during liquefaction increases dramatically, and the values of the associated damping ratio may increase from less than 5% to over 20%. In the present analyses, material damping ratio in the liquefiable soil

stratum is assumed to be equal to 3% without liquefaction and equal to 20% in presence of liquefaction. Given the impermeable nature of the layers above and below the liquefied zone, no pore water pressure dissipation effects are considered.

Regarding Poisson's ratio, the soil is considered fully saturated (S_r = 100%). Accordingly, the apparent compressional wave propagation velocity is V_p = 1500 m/s, i.e. equal to the corresponding wave propagation velocity in water. From Hooke's law, we obtain:

$$\nu = [(V_p/V_s)^2/2–1]/[(V_p/V_s)^2–1] \quad (5)$$

For instance, assuming V_s = 150 m/s without liquefaction and V_{sliq} = 25 m/s with liquefaction, Eq. (5) yields ν = 0.49 and 0.499, respectively. In the analyses reported herein, a uniform value ν = 0.49 is employed corresponding to a nearly incompressible liquefied medium.

Table 1 – Properties of soil layers (values in parenthesis correspond to liquefaction conditions)

Non liquefiable surface crust				Liquefiable sand layer				Non liquefiable base layer			
h_1/B	V_{s1}	β_1	ν_1	h_2/B	V_{s2}	β_2	ν_2	h_3/B	V_{s3}	β_3	ν_3
0.5 1 2	100 250	0.03	0.33	0.5 1 2	150 (25)	0.03 (0.20)	0.49	H/B – $\frac{h_1+h_2}{B}$	300	0.03	0.49

*shear wave propagation velocity V_{si} in m/s, density ρ = 2 Mg/m^3 for all soil layers

With reference to Fig. 1b, the characteristic parameters of each soil layer are the soil thickness, h_i, the shear wave propagation velocity, V_{si}, the mass density, ρ_s, the Poisson's ratio, ν_i, and the material damping, β_{si}. For numerical simulation purposes and for compatibility with previous research [16], it is assumed that the dimensionless ratio of the total soil profile equals H/B = 15, thus, the presence of bedrock does not affect the dynamic response of the footing. Among the aforementioned parameters, the parametric investigation focused upon the effect of the thickness of the liquefied stratum, as well as the thickness and stiffness of the non-liquefiable surface crust (which should meet the bearing capacity requirement under gravity loading). The dimensional analysis that follows justifies the choice of the above critical problem properties. The values of the problem properties considered in the parametric analyses are summarized in Table 1.

A reduction of the independent variables of the problem is possible by means of dimensional analysis. The specific problem involves six major dimensional parameters (M = 6): the thickness of surface crust, h_1, the thickness of liquefiable layer, h_2, the shear wave propagation velocity of non-liquefiable surface crust, V_{s1}, the corresponding velocity of liquefiable layer, V_{s2}, the footing width, B, and the excitation frequency, f. The rest of parameters illustrated in Fig. 1b, including the stiffness of the base layer and the total thickness of the soil profile, are of rather minor importance (have a second order influence on the response) and are not explored parametrically in the ensuing.

In light of the two fundamental dimensions, length [L] and time [T] (N = 2), application of Buckingham's theorem [21] ($M – N$ = 4) leads to four dimensionless ratios controlling the response of the footing. The governing dimensionless groups were selected to be h_1/B, h_2/B, V_{s1}/V_{s2}, $\omega h_1/V_{s1}$. These ratios suffice for fully describing the dynamic impedance of the footing. An extensive parametric study is conducted to elucidate the role of the aforementioned parameters on the impedance functions of the footing.

3. Numerical results

The dynamic impedance of a rigid square footing on liquefiable soil is investigated numerically using simplified cone models based on Strength-of-Materials theory. This method, based on viscoelastic wave propagation in cones, was developed by Wolf and Deeks (implemented in the commercial computer code CONAN [6]) and can be used to determine the dynamic impedance functions of surface or embedded rigid disks. However, various foundation shapes can be also analyzed by considering an equivalent circular radius to match footing area for translational oscillation modes ($R = B/\sqrt{\pi}$), or moment of inertia for rotational oscillation modes ($R = B/\sqrt[4]{(3\pi)}$). With cone models, the complex three-dimensional elastodynamic problem is reduced to a simpler problem described by one-dimensional wave propagation. A soil profile with linear elastic behavior and hysteretic material damping may consist of any number of horizontal layers overlying a halfspace or bedrock. Dynamic impedance is evaluated for any single frequency for vertical, horizontal, rocking and torsional degrees of freedom. The accuracy of the cone model predictions has been verified in a number of studies [6, 22].

3.1 Results for static stiffness

Table 2 presents results for normalized static stiffness of square rigid footings for both pre-liquefaction (V_{s1}/V_{s2} = 0.67 and 1.67) and post-liquefaction (V_{s1}/V_{s2} = 4 and 10) conditions. All main oscillation modes (vertical, horizontal, rocking) are investigated. Static stiffness is normalized with the shear modulus of the surface non-liquefiable soil crust (G) and the width of the footing (B) according to Eq. (1). For convenience, the results are presented in the form of tables and graphs and are expressed in terms of dimensionless quantities.

Table 2 – Normalized static stiffness of square rigid foundations on 3-layer liquefiable soil

		$K_{ij} / (G \times B^m)$											
		Vertical (m=1)				Horizontal (m=1)				Rocking (m=3)			
		V_{s1} / V_{s2}											
		Pre-liquefaction		Post-liquefaction		Pre-liquefaction		Post-liquefaction		Pre-liquefaction		Post-liquefaction	
h_1/B	h_2/B	***0.67***	***1.67***	***4***	***10***	***0.67***	***1.67***	***4***	***10***	***0.67***	***1.67***	***4***	***10***
0.5	***0.5***	6.32	2.97	1.75	1.0	3.08	2.26	1.67	1.31	0.59	0.46	0.39	0.34
	1	5.95	2.65	1.52	0.88	3.02	2.17	1.39	1.18	0.58	0.45	0.37	0.33
	2	5.63	2.38	1.25	0.78	2.95	2.06	1.27	1.08	0.58	0.44	0.36	0.33
1	***0.5***	4.90	3.11	2.39	1.56	2.80	2.39	1.74	1.77	0.53	0.49	0.46	0.44
	1	4.80	2.87	1.98	1.41	2.75	2.32	1.66	1.64	0.52	0.48	0.45	0.44
	2	4.58	2.66	1.70	1.25	2.71	2.27	1.58	1.53	0.52	0.48	0.45	0.44
2	***0.5***	4.10	3.18	2.45	2.30	2.61	2.44	1.85	2.10	0.50	0.50	0.49	0.48
	1	4.13	3.05	2.34	2.08	2.60	2.42	1.82	2.02	0.50	0.49	0.49	0.48
	2	3.96	2.88	2.22	1.85	2.54	2.37	1.79	1.92	0.50	0.49	0.49	0.48

It may be observed that:

a) The stiffness degradation of the liquefiable soil stratum during liquefaction (i.e. the increase of shear wave velocity ratio V_{s1}/V_{s2}) results in a decrease of the static stiffness coefficient, ranging from 28% to 78% for the vertical mode, from 14% to 55% for the horizontal mode and from 2% to 38% for the rocking mode. The highest decrease is observed for initial shear wave velocity ratio V_{s1}/V_{s2} = 0.67. This is anticipated, since a stiff top layer, in contrast with a soft one, can provide sufficient rigidity to the foundation even in presence of a soft underlying soil stratum.

b) The values of post-liquefaction static stiffness coefficient increase as the crust thickness ratio h_1/B increases. This is reasonable if one considers that for a thick top layer the pressure bulb beneath the loaded area (about 1.5 B in diameter) does not extend to the soft underlying liquefied soil.

c) The increase in thickness of liquefiable soil (h_2/B) seems to further reduce the static stiffness coefficient. This is because the stiff non-liquefiable base clayey layer, providing extra rigidity to the foundation, is located in greater depth, thus, reducing stiffening of the foundation response.

3.2 Results for dynamic impedance functions

Results for dynamic impedance functions of square footings on liquefiable three-layer soil profile are depicted in normalized form in Figs. 2 – 4. $\tilde{K}_i$ and $\tilde{C}_i$ refer to post-liquefied dynamic stiffness and damping while K_i and C_i refer to pre-liquefied stiffness and damping values, respectively. Hence, $\tilde{K}_i$ / K_i and $\tilde{C}_i$ / C_i ratios are selected to be examined in order to isolate the influence of liquefaction on the dynamic impedance functions. In the graphs, the stiffness ratio $\tilde{K}_i$ / K_i and damping ratio $\tilde{C}_i$ / C_i are given as a function of the dimensionless frequency ωh_1 / V_{s1}.

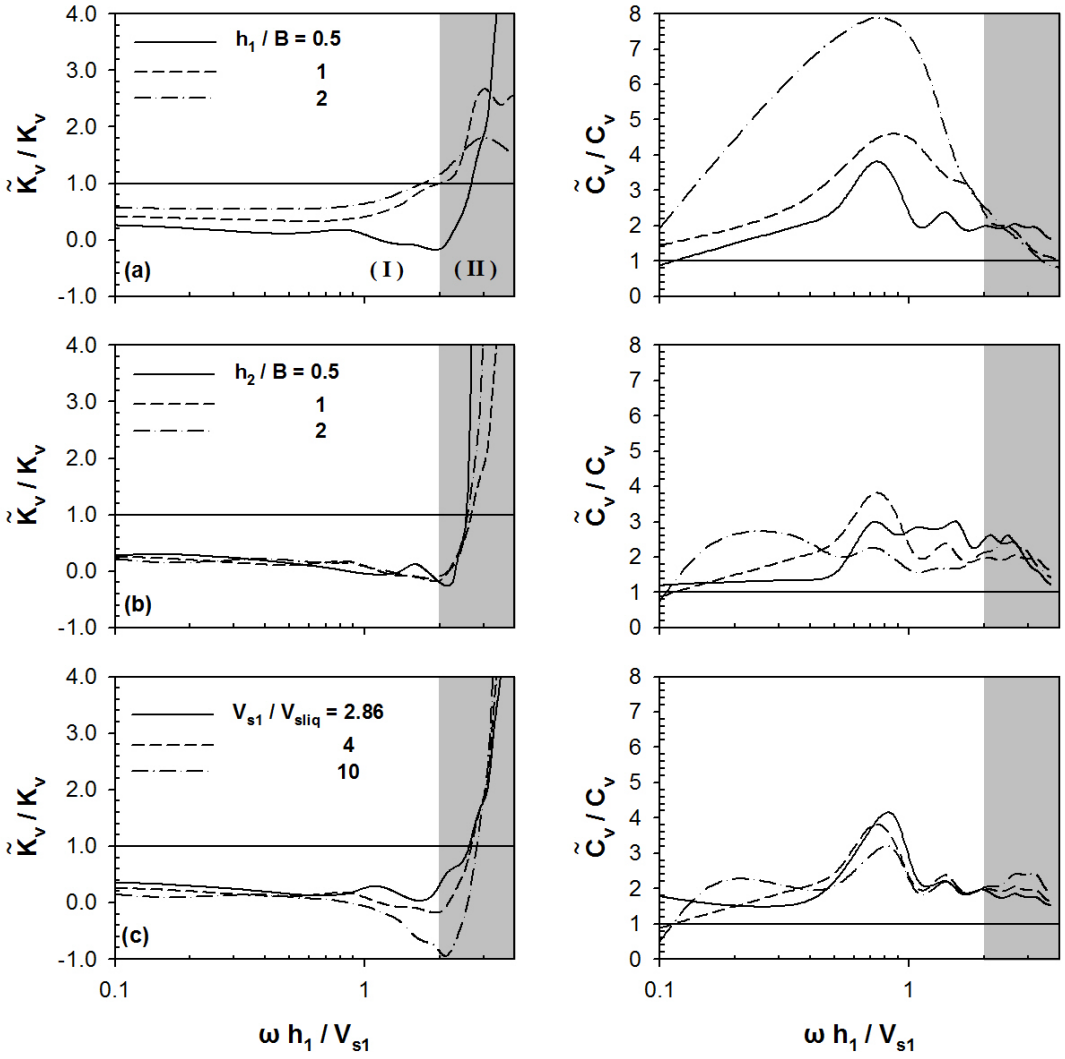

Fig. 2 – Post-liquefied vertical dynamic impedance coefficients of square footing normalized with the corresponding pre-liquefied impedance coefficients; Effect of a) thickness of surface crust, b) thickness of liquefiable soil layer, c) shear wave velocity ratio; h_1/B = 0.5, h_2/B = 1, V_{s1}/V_{s2} = 2/3.

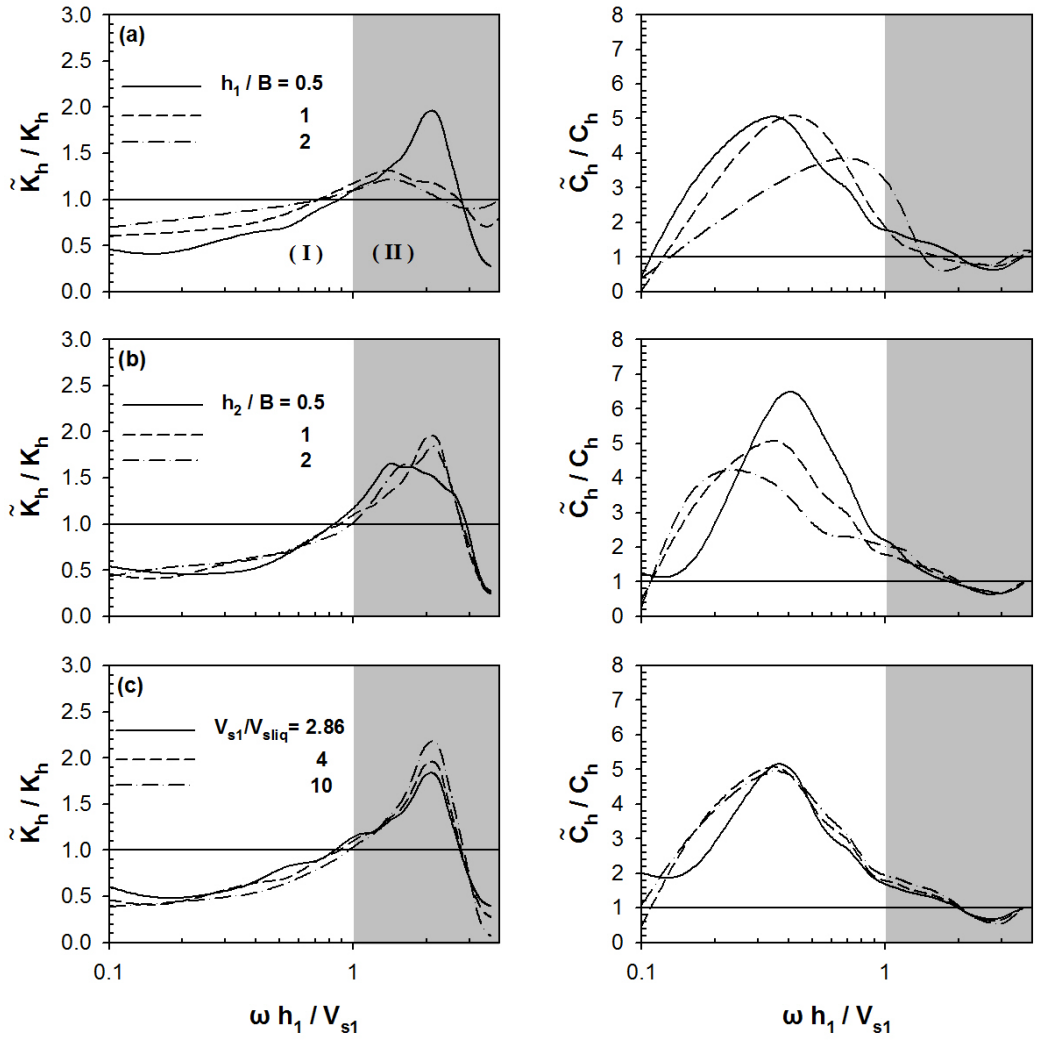

Fig. 3 – Post-liquefied horizontal dynamic impedance coefficients of square footing normalized with the corresponding pre-liquefied impedance coefficients; Effect of a) thickness of surface crust, b) thickness of liquefiable soil layer, c) shear wave velocity ratio; h_1/B = 0.5, h_2/B = 1, V_{s1}/V_{s2} = 2/3.

Inspection of Fig. 2 for the vertical impedance functions reveals the existence of two regions, (I) and (II). Region (I), defined for $\omega h_1 / V_{s1} < 2$, refers to footings having small to moderate width, B = 1 ~ 3 m, (h_1 is comparable to B), profiles with soft soil crust, V_{s1} = 100 ~ 150 m/s, and frequency range f = 0 ~ 10 Hz. On the other hand, region (II) with $\omega h_1 / V_{s1} > 2$ corresponds to large width footings, B > 4 m, profiles with soft to moderate soil crust, V_{s1} = 100 ~ 250 m/s, and high frequency range f > 15 Hz. The same applies for the horizontal and rocking oscillation modes (Figs. 3 and 4), with the only difference being that the bound between these two regions for the horizontal mode is reduced to $\omega h_1 / V_{s1}$ = 1. It is noteworthy that common buildings and structures fall into region (I). It is further observed that the dynamic stiffness is considerably reduced in region (I), while the corresponding dynamic damping ratio $\tilde{C}_i / C_i$ increases well above unity. For region (II), dynamic stiffness seems to amplify exhibiting sharp undulations while $\tilde{C}_i / C_i$ ratio tends to unity.

The following additional noteworthy trends become also evident from Figs. 2 – 4:

(a) The variation in thickness of the surface crust has significant effect on the dynamic impedance functions. Specifically, as the h_1/B ratio decreases dynamic stiffness decreases in region (I). For the second region, the h_1/B ratio does control the undulations in impedance functions.

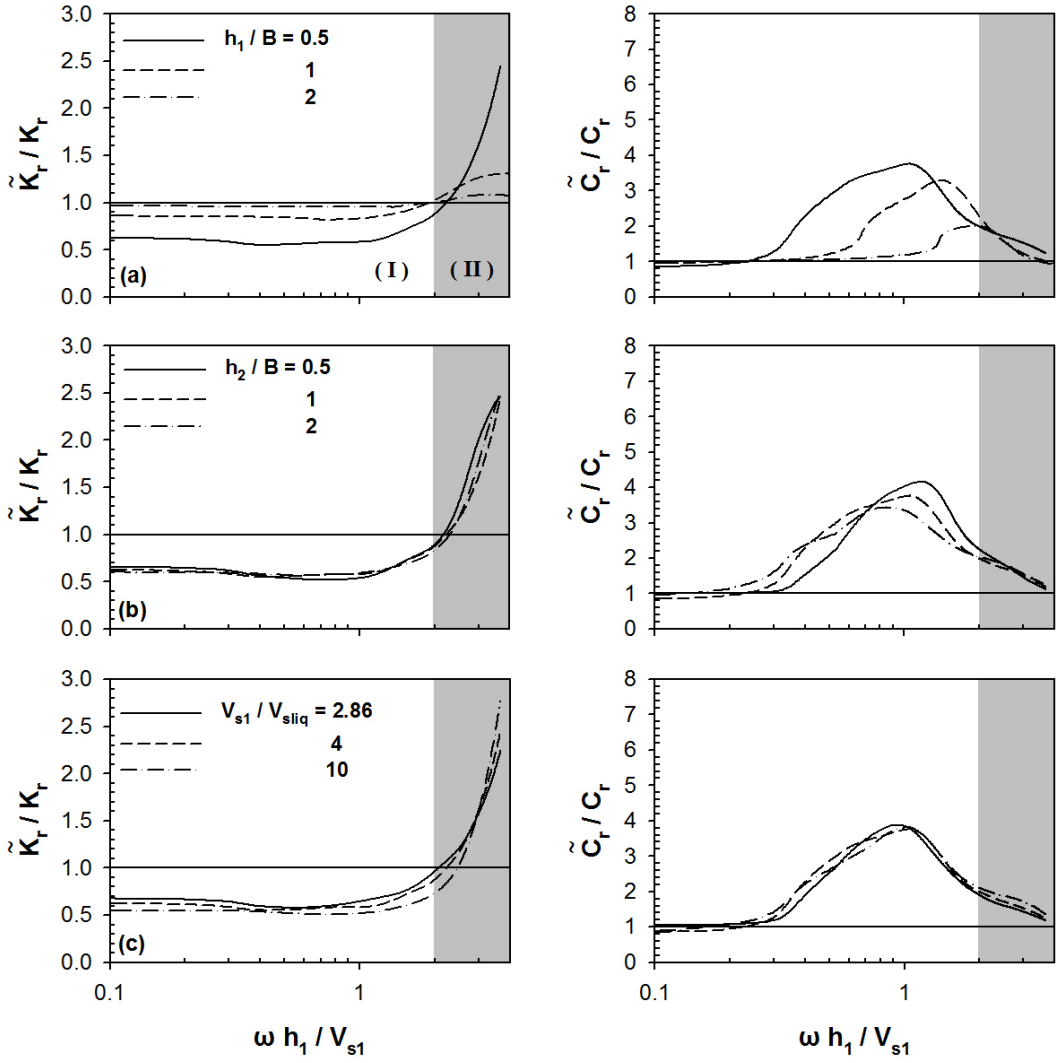

Fig. 4 – Post-liquefied rocking dynamic impedance coefficients of square footing normalized with the corresponding pre-liquefied impedance coefficients; Effect of a) thickness of surface crust, b) thickness of liquefiable soil layer, c) shear wave velocity ratio; h_1/B = 0.5, h_2/B = 1, V_{s1}/V_{s2} = 2/3.

(b) With reference to damping, a significant increase in post-liquefied damping is observed, due to the increase in material damping of the liquefied layer. Increase in the thickness of the surface non liquefiable crust results in amplification of damping for the vertical mode, while the opposite trend is noticed for the other two modes. Interestingly, vertical damping coefficient exhibits a peak at around $\omega h_1 / V_{s1} \approx 0.75$, which suggests development of a kind of resonance at $T_{exc} \approx 2\ T_{s1}$ (i.e. $T_{s1} = 4h_1/V_{s1}$). However, this is not observed for the $\tilde{K}_i / K_i$ ratio.

(c) The change in thickness of the liquefiable soil stratum does not affect the dynamic stiffness of the footing, and the $\tilde{K}_i / K_i$ curves almost coincide. On the contrary, h_2/B ratio seems to affect damping ratio $\tilde{C}_i / C_i$ which increases as the h_2/B ratio decreases, especially in the horizontal mode.

(d) In Figs. 2c – 4c it is noted that the initial shear wave velocity ratio V_{s1}/V_{s2} remains constant (= 2/3) while for the liquefied layer assumed V_{sliq} = 10, 25 and 35 m/s being ~ 7%, 17% and 23% of the initial shear wave velocity. Surprisingly, V_{s1}/V_{sliq} ratio appears to affect only slightly the dynamic impedance functions.

(e) Regarding the vertical dynamic stiffness, it is noted that for some frequencies $\tilde{K}_v$ / K_v ratio admits negative values (with $\tilde{K}_v$ being negative), which suggests that the phase lag between response and excitation is greater than 90°. Moreover, at the high frequency range and for h_1/B = 0.5, dynamic stiffness coefficients are extremely high. It seems that the analysis provides unstable solutions at the high frequency range and further investigation is required to produce robust results.

4. Comparison with BEM analyses

To check the accuracy of the herein reported analyses, a rigorous Boundary Element Method in 3 dimensions implemented in software platform ISoBEM [7] is employed. In this case, the layered medium is solved by considering each soil stratum as a separate homogeneous region, developing BEM equations independently and then assembling and solving the associated set of simultaneous equations by respecting equilibrium and compatibility across a common interface. Note that ISoBEM has been successfully used to study several problems of applied mechanics [23, 24] and soil mechanics [25]. Three-dimensional models simulating a rigid square footing on a three-layer liquefiable soil in ISoBEM were set up to provide comparisons.

In the case of vertical and harmonic oscillations, a comparison is performed between static stiffness coefficients obtained by cone models and ISoBEM analysis. The comparison is summarized in Table 3 as the ratio of values obtained from cone models over the corresponding values obtained from BEM analysis. It is shown that BEM typically predicts higher values for static stiffness. The discrepancies observed are anticipated in light of the complexity of the problem and the extremely low value of shear wave velocity considered for the liquefied stratum (V_{sliq} = 25 m/s). For the pre-liquefied case (V_{s1}/V_{s2} = 0.67), results from the two analyses exhibit differences of less than 10% or so.

Regardless of the observed discrepancies, it is stressed that the percentage of reduction in static stiffness, triggered by the occurrence of liquefaction, is comparable in the two approaches. Hence, rigorous elastodynamic boundary element results verify the significant loss of stiffness of the foundation during liquefaction. From an engineering viewpoint, results are generally comparable and the results from CONAN analyses can be used for a preliminary assessment of the effect of liquefaction on the stiffness of the footing in an equivalent linear sense.

Table 3 – Comparison of vertical and horizontal static stiffness coefficients (BEM vs Cone)

$K_{ij,(BEM)} / K_{ij,(Cone)}$							
		Vertical			**Horizontal**		
		V_{s1} / V_{s2}					
		0.67	**4**	**10**	**0.67**	**4**	**10**
h_1/ B	**h_2/ B**	BEM / Cone					
0.5	0.5	1.11	1.56	1.26	1.16	1.23	1.11
	1	1.10	1.11	0.86	1.16	1.32	1.13
	2	1.08	0.84	0.59	1.16	1.28	1.14
1	0.5	1.06	1.38	1.25	1.13	1.38	1.08
	1	1.05	1.31	0.98	1.13	1.33	1.10
	2	1.06	1.06	0.84	1.11	1.28	1.12
2	0.5	1.00	1.46	1.18	1.14	1.41	1.10
	1	0.98	1.41	1.11	1.12	1.36	1.11
	2	1.01	1.23	0.98	1.14	1.32	1.14

Fig. 5 depicts a comparison between dynamic stiffness and damping coefficients obtained by means of Cone and BEM solutions. For the purposes of this discussion, the case where h_1/B = 1, h_2/B = 1 and V_{s1}/V_{s2} = 4

is depicted. Spring coefficient k_{ij} and dashpot coefficient c_{ij} are plotted, in accordance with Eq. 4, against the dimensionless frequency a_0, i.e., $\omega R/V_{s1}$ with $R = B/\sqrt{\pi}$ being the equivalent circular radius, stemming from the cone solution, and $\omega(B/2)/V_{s1}$ for results obtained using the boundary element method. It is observed that agreement between Cone model predictions and BEM results is quite good.

For vertical oscillations, CONAN predictions for spring and dashpot coefficients are in satisfactory agreement with the rigorous BEM results. Curves exhibit similar trends, except perhaps for $\tilde{k}_v$ in the high frequency range. For horizontal oscillations, there is a consistent over-prediction of dynamic stiffness from the Cone method at all frequencies. However, the curves exhibit the same trend. For dashpot coefficient, accord is better.

It should be pointed out that, the agreement of the two independent analyses does not ensure that the results reflect the dynamic behavior of the liquefiable soil-footing system and, hence, experimental validation is badly needed.

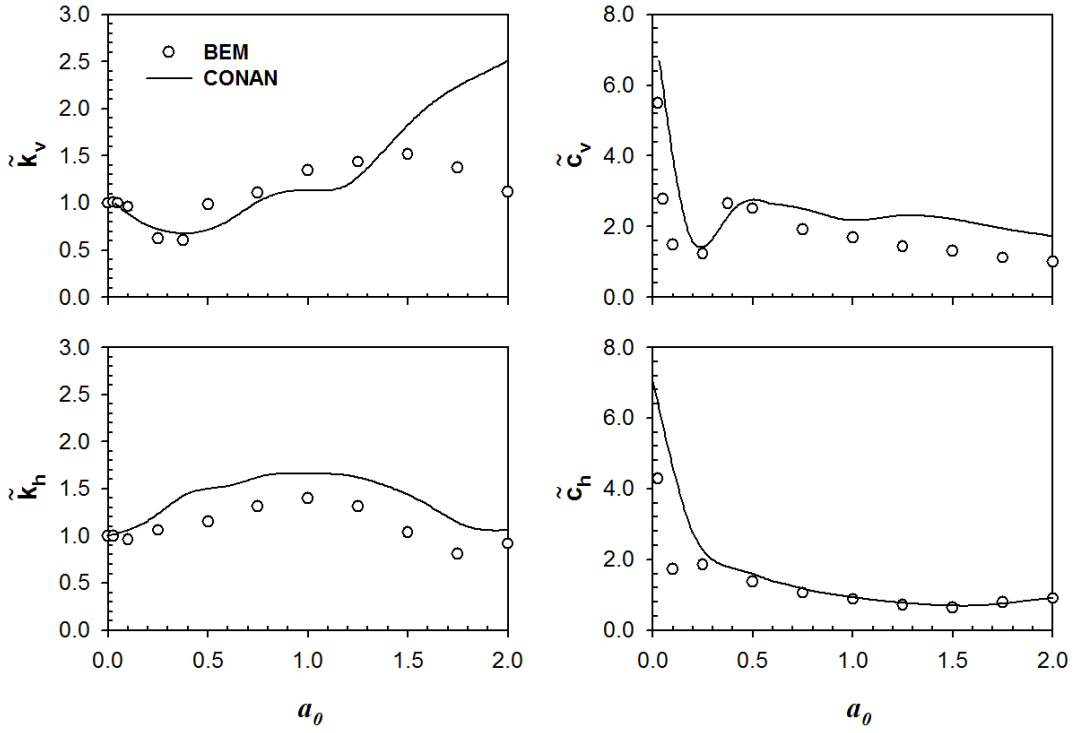

Fig. 5 – Comparison of vertical and horizontal dynamic impedance functions (BEM vs Conan); $h_1/B = 1$, $h_2/B = 1$, $V_{s1}/V_{s2} = 4$

5. Conclusions

A parametric investigation was conducted using elastodynamic methods to explore the dynamic response of a surface rigid square footing on a three-layer liquefiable soil under harmonic excitation. Although liquefaction is a strongly non-linear phenomenon and advanced methods are necessary for a rigorous treatment of the problem, elastodynamic analyses, based on proper assumptions for the values for the shear wave velocity and material damping of the liquefied layer, can shed light into the physics of dynamic impedance functions of footings.

The following conclusions could be drawn from the investigation at hand:

a) Results obtained from simplified cone models (CONAN software) compare well against more rigorous BEM results (ISoBEM software) for the pre-liquefied case. Nevertheless, for the post-liquefied case results deviate considerably, perhaps owing to the extremely low value assumed for the shear wave velocity of the liquefied

stratum. From a geotechnical engineering viewpoint, results are generally comparable and both methods demonstrate a significant decrease in footing stiffness accompanied by a considerable increase in damping due to liquefaction. In this light, the Cone method seems to be appropriate for a preliminary assessment of the problem at hand.

b) Static stiffness of the footing is reduced dramatically under liquefied conditions. The decrease ranges from 28% to 78% for the vertical mode, from 14% to 55% for the horizontal mode, and from 2% to 38% for the rocking mode.

c) Key parameters of the problem emerging from this study are the dimensionless thickness of the surface non-liquefiable crust h_1/B, the dimensionless thickness of the liquefiable soil layer h_2/B, the relative stiffness of the surface layer V_{s1}/V_{s2}, and the dimensionless excitation frequency $\omega h_1 / V_{s1}$.

d) The influence of liquefaction on the dynamic impedance functions is investigated through the dimensionless ratios $\tilde{K}_i / K_i$ and $\tilde{C}_i / C_i$. Results demonstrate the existence of two distinct regions. For the low frequency range and footings used for the foundation of common structures ($\omega h_1/V_{s1} < 1$~2), significant reduction is observed in dynamic stiffness accompanied by a considerable increase in damping. Outside that range ($\omega h_1 / V_{s1} > 2$), dynamic stiffness exhibits sharp undulations while damping ratio $\tilde{C}_i / C_i$ tends to unity.

e) h_1/B ratio does control the undulations of the impedance functions in any of the three oscillation modes. Naturally, static stiffness increases with increasing h_1/B.

f) An increase in h_2/B ratio results in a decrease in static stiffness but it does not affect considerably the dynamic stiffness coefficient. However, damping ratio $\tilde{C}_i / C_i$ seems to be more sensitive to this ratio.

g) Remarkably, V_{s1}/V_{sliq} ratio seems to be of secondary importance since it only slightly affects the dynamic impedance functions of the footing.

h) Finally, experimental validation of the above findings is needed to apply results to field problems.

6. Acknowledgements

This research was co-financed by the European Union (European Social Fund – ESF) and Greek national funds through the Operational Program "Education and Lifelong Learning" of the National Strategic Reference Framework (NSRF)-Research Funding Program: THALES. Investing in knowledge society through the European Social Fund. The help of Professors Demosthenes Polyzos and Dimitri Beskos of UPatras in making available ISoBEM software to the authors is gratefully acknowledged, as well as the help of Professor Stephanos Tsinopoulos of the Technological Institute of Patras in using the software.

7. Copyrights

8. References

[1] Karamitros D., Bouckovalas G., Chaloulos Y. (2013a): Insight into the seismic liquefaction performance of shallow foundations. *Journal of Geotechnical and Geoenvironmental Engineering*, 139, 599-607.

[2] Karamitros D., Bouckovalas G., Chaloulos Y. (2013b): Seismic settlements of shallow foundations on liquefiable soil with a clay crust, *Soil Dynamics and Earthquake Engineering*, 46, 64-76.

[3] Karamitros D., Bouckovalas G., Chaloulos Y., Andrianopoulos K., (2013c): Numerical analysis of liquefaction-induced bearing capacity degradation of shallow foundations on a two-layered soil profile. *Soil Dynamics and Earthquake Engineering*, 44, 90-101.

[4] Acacio A., Kobayashi Y., Towhata I., Bautista R., Ishihara K. (2001). Subsidence of building foundation resting upon liquefied subsoil; Case studies and assessment, *Soils and Foundations*, 41(6), 111-128

[5] Sitar N., Hausler E. (2012). Influence of Ground Improvement on Liquefaction Induced Settlements: Observations from Case Histories and Centrifuge Experiments, Invited Lecture presented to the Korean Geotechnical Society, Seoul, Korea, March 22 2012.

[6] Wolf J.P., Deeks A.J. (2004): *Foundation Vibration Analysis: A Strength-of-Materials Approach.* Elsevier, Oxford, UK

[7] ISoBEM: Boundary Element Method Package. http://bemsands.com, 2012.

[8] Wong HL, Luco JE. (1985): Tables of impedance functions for square foundation on layered media. *Soil Dynamics and Earthquake Engineering*, 4(2),64–81.

[9] Pais A., Kausel E. (1988): Approximate formulas for dynamic stiffnesses of rigid foundations. *Soil Dynamics and Earthquake Engineering*, 7(4), 213–227.

[10] Gazetas G. (1991): Formulas and charts for impedances of surface and embedded foundations. *Journal of Geotechnical Engineering*, 117 (9), 1363-1381.

[11] Meek JW, Wolf JP. (1992): Cone models for soil layer on rigid rock. *Journal of Geotechnical Engineering, ASCE*,118,686–703.

[12] Vrettos C. (1999): Vertical and rocking impedances for rigid rectangular foundations on soils with bounded non-homogeneity. *Earthquake Engineering and Structural Dynamics*, 28 (12), 1525-1540.

[13] Mylonakis G., Nikolaou S., Gazetas G. (2006): Footings under seismic loading: Analysis and design issues with emphasis on bridge foundations. *Soil Dynamics and Earthquake Engineering*, 26 (9), 824-853.

[14] Ahmad S., Rupani A. (1999): Horizontal impedance of square foundation in layered soil. *Soil Dynamics and Earthquake Engineering*, 10.1016/S0267-7261(98)00028-1, 59-69.

[15] Miwa S., Ikeda T. (2006): Shear modulus and strain of liquefied ground and their application to evaluation of the response of foundation structures. *Structural Engineering/Earthquake Engineering, JSCE*, 23 (1), 167-179.

[16] Theocharis A. (2011): Numerical analysis of liquefied ground response under harmonic seismic excitation-Variable thickness of liquefied layer. *Diploma thesis*, NTUA, Greece.

[17] ASCE. 2010. *Minimum Design Loads for Buildings and Other Structures*. ASCE/SEI Standard 7-10.

[18] FEMA, 2009, *NEHRP Recommended Seismic Provisions for New Buildings and Other Structures*, FEMA P-750/2009 Edition, prepared by the Building Seismic Safety Council of the National Institute of Building Sciences for the Federal Emergency Management Agency, Washington, D.C.

[19] NIST (2012). *Soil-Structure Interaction for Building Structures*, GCR 12-917-21, prepared by the NEHRP Consultants Joint Venture, a partnership of the Applied Technology Council and the Consortium for Universities for Research in Earthquake Engineering, for the National Institute of Standards and Technology, Gaithersburg, MD.

[20] Anoyatis G., Mylonakis G. (2012): Dynamic Winkler modulus for axially loaded piles. *Geotechnique*, 62, 521-536.

[21] Buckingham E. (1914): On physically similar systems; illustrations of the use of dimensional equations. *Physical Review*, 4 (4), 345-376.

[22] Hiltunen D., Dunn P., Toros U. (2007): Cone model predictions of dynamic impedance functions of shallow foundations. *4th International Conference on Earthquake Geotechnical Engineering ICEGE*, Thessaloniki, Greece.

[23] Polyzos D., Tsinopoulos S., Beskos D. (1998): Static and dynamic boundary element analysis in incompressible linear elasticity. *European Journal of Mechanics A/Solids*, 17 (3), 515-536.

[24] Tsinopoulos S., Kattis S., Polyzos D., Beskos D. (1999): An advanced boundary element method for axisymmetric elastodynamic analysis, *Computer Methods in Applied Mechanics and Engineering*, 175, 53-70.

[25] Heidarzadeh B., Mylonakis G., Stewart JP. (2015): Stresses beneath dynamically applied vertical point loads. 6th *International Conference on Earthquake Geotechnical Engineering ICEGE*, Christchurch, New Zealand.